

# The Structure and Properties of Copper Oxide and Copper Aluminum Oxide Coatings Prepared by Pulsed Magnetron Sputtering Of Powder Targets

E.M. Alkoy<sup>1)</sup>, Rika Suwana Budi<sup>2)</sup>, Liu Feng Gouw<sup>1)</sup>

<sup>1)</sup>Beihang University of Aeronautics and Aerospace, P.R China, 100191

<sup>2)</sup>National Institute of Aeronautics and Space, Republic of Indonesia

**Abstract:** The development of p-type semiconductors is one of the key technologies for p–n junction-based devices, such as diodes, transistors and light-emitting diodes. Copper oxide and copper aluminum oxide (CuAlO<sub>2</sub>) coatings are known to show p-type conductivity and, as a consequence, these materials are attracting increasing attention. In this study, therefore, various copper oxide and CuAlO<sub>2</sub> films were deposited by pulsed magnetron sputtering from loosely packed powder targets, formed from either Cu<sub>2</sub>O powder alone, or blends of Cu<sub>2</sub>O and Al<sub>2</sub>O<sub>3</sub> powders, in a rig specifically designed for the purpose. The coatings were deposited at varying partial pressures of oxygen and then annealed at atmospheric pressure. The optical, electrical and structural properties were determined using a range of techniques including spectrophotometry, four-point probe, scanning electron microscopy and X-ray diffraction. Analysis of the films showed that, in the former case, crystalline Cu<sub>2</sub>O and CuO structures could be produced, depending on the oxygen partial pressure during deposition and the post-deposition annealing conditions. The deposited Cu<sub>2</sub>O films were found to have a very high optical transmittance in the visible range with up to 95% transmission. In comparison, the CuO films showed lower transmittance in the visible range, but greater transmittance in the IR range. The optical band gaps obtained from the transmittance and reflectance measurements were 2.44 and 1.78 eV for Cu<sub>2</sub>O and CuO, respectively. The CuAlO<sub>2</sub> coatings were also found to be crystalline, with optical and electrical properties again dependent on the deposition and annealing conditions. The direct deposition of transparent conductive oxide films from loosely packed powder targets by pulsed magnetron sputtering is a novel, highly versatile technique for the deposition of this type of material.

**Key Words:**

## 1. Introduction

There are many well-known transparent conductive oxide (TCO) materials and their doped derivatives. TCOs such as electron doped ZnO, In<sub>2</sub>O<sub>3</sub>, SnO<sub>2</sub> are n-type materials and are used, for example, as transparent electrodes in flat panel displays, solar cells, and touch panels<sup>1</sup>. These materials need to have good optical transparency and electrical conductivity for their applications. There are, however, new TCOs with p-type conductivity. Indeed, the development of p-type transparent conducting oxides is one of the key technologies for p–n junction-based oxide devices, such as diodes, transistors and light-emitting diodes<sup>2</sup>.

Oxides of copper and copper aluminum oxide (CuAlO<sub>2</sub>) are known to show p-type conductivity and are attracting renewed interest as promising TCO materials for the fabrication of a range of devices. There are two common forms of copper oxide: cupric oxide or tenorite (CuO) and cuprous oxide or cuprite (Cu<sub>2</sub>O). CuO is a p-type semiconductor with a band gap of 1.9–2.1 eV and a monoclinic structure<sup>3,4</sup>. Cu<sub>2</sub>O is also a p-type semiconductor with a band gap of 2.1–2.6 eV and a cubic structure<sup>3,5</sup>. These materials have unique features such as their low cost, non-toxicity, the abundant availability of copper, a theoretical solar cell efficiency of 18% and relatively simple formation of the oxide layer<sup>6</sup>. Deposition of copper oxide thin films has been reported by various techniques, such as reactive magnetron sputtering<sup>4</sup>, reactive evaporation<sup>5</sup>, RF sputtering<sup>6</sup>, ion beam sputtering<sup>7</sup>, plasma evaporation<sup>8</sup>, sol–gel<sup>9,10</sup>, molecular beam epitaxy<sup>11</sup> and CVD<sup>12</sup>.

Kawazoe et al.<sup>13</sup> also reported p-type conductivity in CuAlO<sub>2</sub> thin films produced by the laser ablation method and the fabrication of p–n hetero junctions with other n-type TCOs<sup>14</sup>. The synthesis and characterization of CuAlO<sub>2</sub> films has also been investigated by Banerjee et al.<sup>15,16</sup> and Banerjee and Chattopadhyay<sup>17</sup> via the DC sputtering method, by Yanagiet al.<sup>1</sup> via the pulsed laser deposition method and by Tonooka et al.<sup>2</sup> via dip-coating methods. Other p-type TCO thin films that are reported in the literature are CuGaO<sub>2</sub> and SrCu<sub>2</sub>O<sub>2</sub><sup>15</sup>.

This study was conducted to investigate the deposition of copper oxide and copper aluminum oxide

thin films by the pulsed magnetron sputtering of loosely packed (as opposed to sintered, or pressed) powder targets. In the former case, the sputtering target was formed from  $\text{Cu}_2\text{O}$  powder and the different phases of copper oxide were prepared by varying the oxygen flow rate during deposition, and by different post-deposition annealing treatments. In the latter case, sputtering took place from a powder target composed of copper oxide ( $\text{Cu}_2\text{O}$ ) and alumina ( $\text{Al}_2\text{O}_3$ ) powders mixed in 1:1 = Cu : Al atomic ratio. The advantages offered by this approach over conventional DC and RF sputtering from solid metallic, or ceramic targets are that, since oxide powders are used, no reactive process control equipment is required, there is no need for RF matching networks, the powder is loosely packed, so target cracking issues are avoided and the target composition can be readily varied. Furthermore, the starting materials are relatively cheap and, since the powder can be simply re-distributed across the target, no permanent racetrack is formed and material utilisation is very high, compared to a solid target. This is a highly flexible deposition technique, which has been successfully utilized to deposit a range of TCO and other coating materials, including doped zinc oxides<sup>18-20)</sup>, indium tin oxide<sup>21)</sup>, copper indium diselenide<sup>22,23)</sup> and chromium diboride<sup>24)</sup>.

## 2. Experimental

Copper oxide and copper aluminum oxide thin films were deposited on glass microscope slides by pulsed magnetron sputtering from powder targets in a rig specifically designed for this technique<sup>18-24)</sup>. The copper oxide target was formed from 99% pure  $\text{Cu}_2\text{O}$  powder (Alfa Aesar), whilst the copper aluminum oxide target was formed from a 1:1 mole ratio mixture of 99%  $\text{Cu}_2\text{O}$  powder and 99.99%  $\text{Al}_2\text{O}_3$  powder (Alfa Aesar). For each material, the average particle size was 50 nm. The powder blends were made by mixing the appropriate quantities of  $\text{Cu}_2\text{O}$  and  $\text{Al}_2\text{O}_3$  powders in a rotating drum for several hours. In both cases, a charge of approximately 60 g of powder was evenly distributed across the surface of a copper backing plate on the magnetron to form a target. The backing plate had been recessed to a depth of 2mm to allow a reasonable target thickness to be produced. The powder was lightly tamped down to produce a uniform thickness and surface to the target. No further processes were involved in target production.

The glass substrates were cleaned with acetone and air-dried before loading in the chamber. Prior to deposition, the substrates were also RF sputter cleaned at 150W for 15 mins using an Advanced Energy RFX 600 power supply. During deposition, the magnetron discharge was pulsed at 350 kHz using a 10 kW Advanced Energy Pinnacle Plus power supply, operating in current regulation mode (target current = 2 A), at 50% duty (pulse off time = pulse-on time = 1.4 ms). Based on previous experience of this system<sup>18-24)</sup>, these deposition parameters were chosen to produce stable, arc-free operating conditions. For the copper oxide runs, the argon flow rate was kept constant at 25.5 sccm for all runs, whilst the oxygen flow rate was varied from 0 to 8 sccm. For the copper aluminum oxide runs, the argon and oxygen flow rates were varied to allow deposition in an argon only atmosphere, an Argon to oxygen ratio of 3:1 and an argon to oxygen ratio of 3:2. The sputtering conditions that were used in the experiments are given in Table 3.1.1. Both 'thick' (60 min deposition time) and 'thin' (10 min deposition time) coatings were produced under each set of conditions to suit specific analytical techniques. During sputtering, no problems such as out gassing, or arcing were observed at either of the targets prepared during this study. Post deposition, the coated slides were sectioned to provide a number of identical samples of each coating. An as-deposited sample was held back, with the remainder being annealed in a box furnace for 1-4 h under atmospheric conditions at various temperatures in the range 350-550 °C.

The structure, morphology, electrical and optical properties of the films were examined using X ray diffraction (Siemens D5000 in  $\theta$  -  $2\theta$  mode with  $\text{CuK}_\alpha$  radiation), scanning electron microscopy (Cambridge Stereo scan 600 and Philips XL30 Field Emission), four point probe resistivity measurements and UV-Vis spectrophotometry (Aquila Instruments nkd 8000, spectral range 350-1000 nm), respectively.

### 3. Results

#### 3.1. Structure and Morphology

The slides coated for 60 min were fractured, mounted and gold coated to allow structural and morphological analysis by scanning electron microscopy. Fig. 3.1.1.a and 3.1.1.b are low-resolution SEM micrographs of the fracture sections of copper oxide coating CO1 and copper aluminum oxide coating, CAO1, respectively, which are typical examples from each batch of coatings. As can be seen, the coatings have dense columnar structures, smooth surfaces and no visible defects. At low resolution, no morphological changes were observed in the coatings after annealing. However, at higher resolution, it was apparent that significant grain growth had occurred in the coatings annealed at high temperatures for extended times. An example of this effect is shown in Figs. 3.1.2.a and b, which compare high-resolution surface SEM micrographs of copper oxide coating CO1 annealed at 350 °C for 1 h and 550 °C for 4 h, respectively.

**Table 3.1.1.** Experimental processing conditions for copper oxide (COx) and copper aluminium oxide (CAOx) coatings

Sample code	Coating time (min)	Coating pressure (Pa)	Argon flow (sccm)	Oxygen flow, (sccm)
CO1	60	0.20	25.5	0
CO2	10	0.20	25.5	0
CO3	60	0.23	25.5	4
CO4	10	0.23	25.5	4
CO5	60	0.27	25.5	8
CO6	10	0.27	25.5	8
CAO1	60	0.20	24	0
CAO2	10	0.20	24	0
CAO3	60	0.27	24	8
CAO4	10	0.27	24	8
CAO5	10	0.27	15	10

Deposition rates were estimated from the fracture section micrographs, and were found to be of the order of 12 nm/min for the copper oxide coatings deposited in an argon only atmosphere and 5–6 nm/min for those deposited in argon/oxygen atmospheres, i.e. in what is effectively an active sputtering process. The rates for the copper aluminum oxide coatings were somewhat lower, being only 4 and 1.6 nm/min, respectively, for the two deposition environments. This may, perhaps, reflect the lower sputtering yield of alumina, in comparison with cuprite. XRD analysis revealed significant variations in the crystallographic structure and phase composition of the films produced from both target types, depending on both the deposition conditions and annealing conditions.

For the copper oxide target, it was found that the films produced with no additional oxygen flow were phase-pure cuprite ( $\text{Cu}_2\text{O}$ ) with a single strong diffraction peak at  $2\theta = 41.56^\circ$  ( $d = 2.17\text{\AA}$ ) indicating a fully (2 0 0)-oriented film (Fig. 3a). Following a post-deposition air annealing of the films at 350 °C for 1 h, two small peaks appear at  $2\theta = 35.32^\circ$  and  $43.041^\circ$  ( $d = 2.538$  and  $2.099\text{\AA}$ , respectively), corresponding to ( $\bar{1}$  1 1) and ( $\bar{1}$  1 2) planes of the monoclinic tenorite structure (CuO) (Fig. 3b). Increasing the annealing temperature to 450 °C resulted in further transformation of the cuprite phase into tenorite with the intensity of (2 0 0) peak of the  $\text{Cu}_2\text{O}$  decreasing (Fig. 3.2.1.c). It also yielded enhanced crystallization of the tenorite phase with increasing intensity of ( $\bar{1}$  1 1) peak and additional peaks appearing at  $2\theta = 38.89^\circ$  and  $53.321^\circ$  with  $d = 2.313$  and  $1.716\text{\AA}$ , belonging to the (2 0 0) and (0 2 0) planes of CuO. Annealing at 550 °C for 1 h resulted in full transformation from cuprite to tenorite (Fig. 3.2.1.d) and increasing the annealing time further to 4 h caused only an increase in the intensity of the ( $\bar{1}$  1 1) peak and a decrease in the intensity of the (0 2 0) peak (Fig. 3.2.1.e).

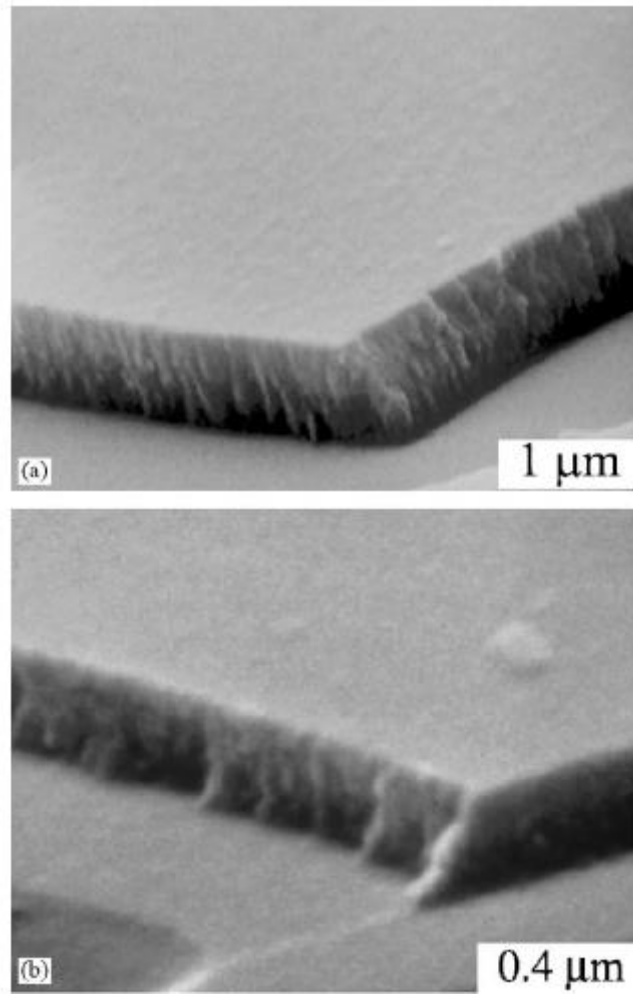


Fig. 3.1.1. (a) SEM micrograph of the fracture section of copper oxide coating CO1, deposited in an argon-only atmosphere for 60 min and (b) SEM micrograph of the fracture section of copper aluminum oxide coating CAO1, deposited in an argon only atmosphere.

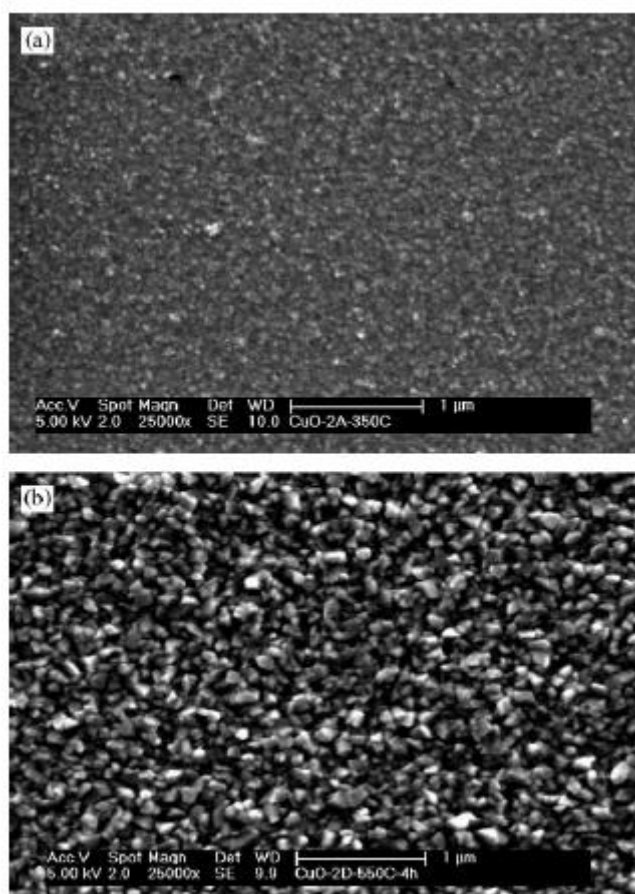


Fig. 3.1.2. High-resolution SEM micrograph of the surface of copper oxide coating CO1 after annealing at: (a) 350 °C for 1 hand (b) 550 °C for 4 h.

Films deposited under 4 and 8 sccm oxygen flows showed no evidence of the  $\text{Cu}_2\text{O}$  phase, but were found to consist of phase-pure  $\text{CuO}$ , with the main diffraction peaks corresponding to the  $(\bar{1} 1 1)$ ,  $(2 0 0)$  and  $(0 2 2)$  planes for both oxygen flow rates (Figs. 3.2.2.a and 3.2.2.c). The main influence of the oxygen flow rate was to increase the intensity of the peaks in the 8 sccm case (Fig. 3.1.4.c), which may imply a higher degree of crystallization. The effect of post-deposition annealing on the  $\text{CuO}$  thin films produced under both oxygen flow rates was further crystallization, with the additional appearance of the  $(0 2 0)$  peak (Fig. 3.2.2.b).

XRD spectra for the  $\text{CuAlO}_2$  coatings deposited in an argon only atmosphere showed only a single peak at  $2\theta = 37.50^\circ$ , before and after annealing at 550 °C for 1 h, as shown in Figs. 3.2.3.a and 3.2.3.b. It is most likely that this peak corresponds to diffraction from the  $(0 1 2)$  plane of the delafossite structure, although since this peak is relatively broad, it could be an unresolved doublet of the  $(1 0 1)$  and  $(0 1 2)$  peaks, as has been reported elsewhere<sup>13</sup>. Films deposited with additional oxygen showed essentially the same structure, although the intensity of the single peak was considerably reduced, which may simply be due to the lower thickness of these films (approximately 100 nm, compared to 245 nm for the argon only films).

### 3.2. Optical Properties

The transmittance of coating CO2 (deposited in an argon only atmosphere for 10 min), over the spectral range 350–1000 nm, is shown in Fig. 3.2.1., both in the as-deposited state and after annealing at 350, 450 and 550 °C for 1 h. These results support the XRD analysis by confirming the transformation of the structure from  $\text{Cu}_2\text{O}$  to  $\text{CuO}$  during the annealing process. The as deposited

$\text{Cu}_2\text{O}$  films display a high transmission in the visible range (peak transmission = 95% at 620nm for a film thickness of 100 nm), decreasing in the IR range, and as the film transforms into  $\text{CuO}$ , visible transmittance decreases significantly, whilst the IR transmittance rises. A similar behaviour with phase transformation as a result of air annealing was also observed by Nair et al.<sup>9</sup> and is consistent with the solar absorbance applications of the tenorite films<sup>12</sup>. However, there is a slight difference between the XRD and optical transmittance results in terms of the temperature at which this transformation is complete. In bulk form the conversion of cuprite into tenorite is reported to take place at 400 °C<sup>9</sup>. However, Fig. 3.2.1.c shows the existence of a mixed phased film with  $\text{Cu}_2\text{O}$  still persisting after annealing for 1 h at 450 °C, whereas the optical transmittance measurements given in Fig. 6 indicate that transformation is complete after annealing at 450 °C. Similar disagreements between the XRD data and optical measurements have been observed elsewhere<sup>4</sup> on post-deposition air annealing of cuprite films and can be explained from a kinetic point of view. The XRD data is taken from a 700nm thick film whereas the optical measurements are taken from a 100nm thick film. Although the conversion of cuprite into tenorite can start to take place at 400 °C, it proceeds by the diffusion of oxygen into the films, and as the film gets thicker, it will require more time for full conversion.

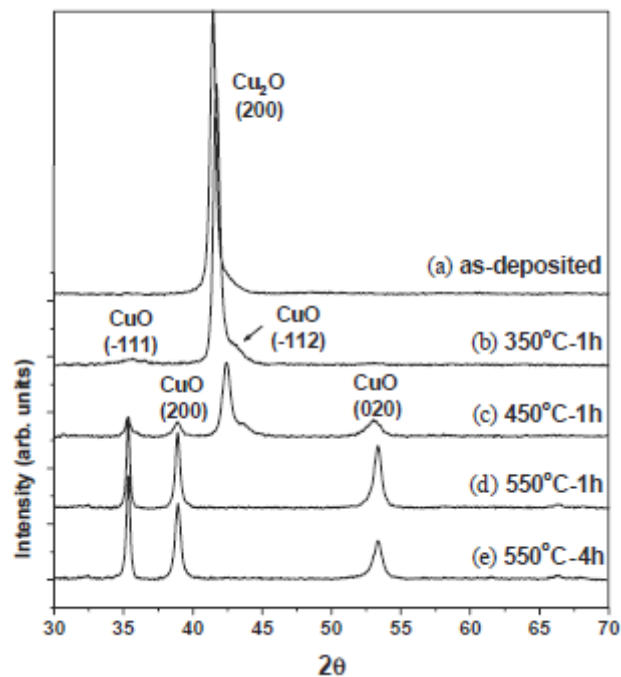


Fig. 3.2.1. (a)–(e)  $\theta$ - $2\theta$  XRD spectra of copper oxide coating CO1, deposited in an argon-only atmosphere, and post deposition annealed at various temperatures and times.

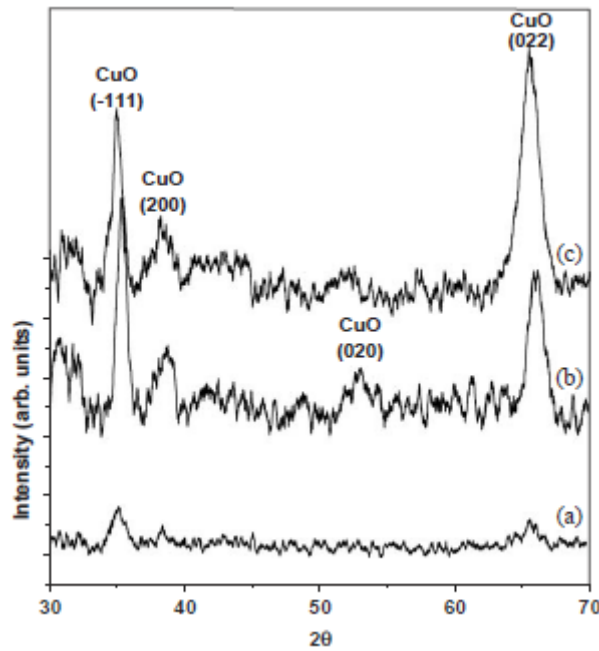


Fig. 3.2.2. (a)–(c)  $\theta$ - $2\theta$ XRD spectra of copper oxide films deposited with additional oxygen flows of: (a) 4 sccm, as deposited (coating CO3); (b) 4 sccm, post-deposition annealed at 450 °C; (c) 8 sccm, as-deposited (coating CO5).

Fig. 3.2.5 compares the optical transmittance of the films deposited with various oxygen flow rates and annealed in air at 550 °C for 1 h. According to the XRD results, all three films are phase-pure tenorite (CuO). It is presumed, therefore, that the observed differences in their optical transmittance behavior must be related to the differences in the crystallinity and the crystallite sizes of the films. Figs. 3 and 4 imply that the tenorite films that are obtained through conversion of cuprite films by post-deposition air annealing have a higher degree of crystallinity and a more ordered structure compared to the reactively deposited tenorite films. Further investigation would be required to confirm this hypothesis.

The optical band gap ( $E_g$ ) of the copper oxide thin films are estimated from the optical transmittance,  $T(\%)$  and reflectance,  $R(\%)$  spectra. Initially, optical absorption coefficients ( $\alpha$ ) of the films were calculated using the following equations <sup>9)</sup> :

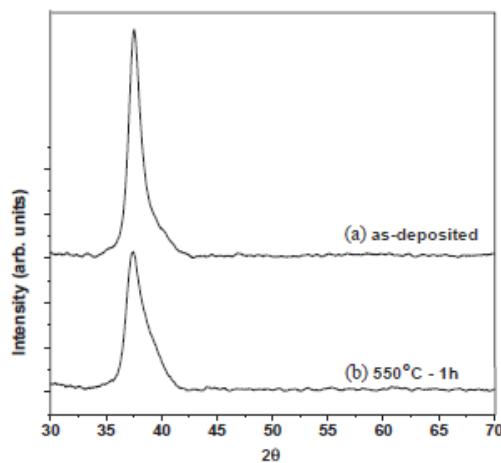


Fig. 3.2.3. (a) and (b)  $\theta$ - $2\theta$  XRD spectra of CuAlO<sub>2</sub> coating CAO1 deposited in an argon-only atmosphere : (a) as-deposited and (b) post-deposition annealed at 550 °C for 1 h.

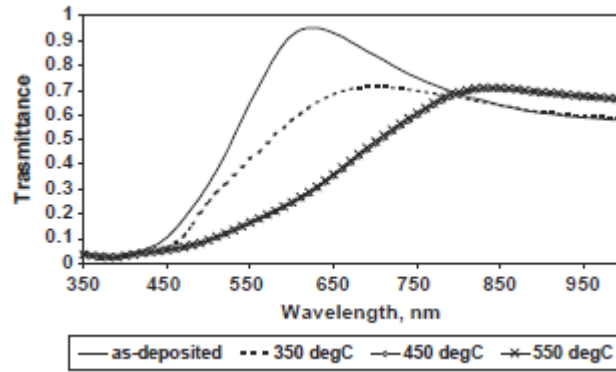


Fig. 3.2.4. Optical transmittance spectra of copper oxide thin films (coating CO<sub>2</sub>) deposited in an argon-only atmosphere and post deposition annealed at various temperatures for 1 h.

$$T_{corr}(\%) = \frac{100T(\%)}{100 - R(\%)} \quad (1.)$$

$$\alpha = \frac{1}{d} \left[ \ln \frac{100}{T_{corr}(\%)} \right] \quad (2.)$$

where  $T_{corr}(\%)$  is the transmittance corrected for reflection losses at the air–film and film–substrate interface, and  $d$  is the film thickness. The optical band gap ( $E_g$ ) can be obtained from the following equation:

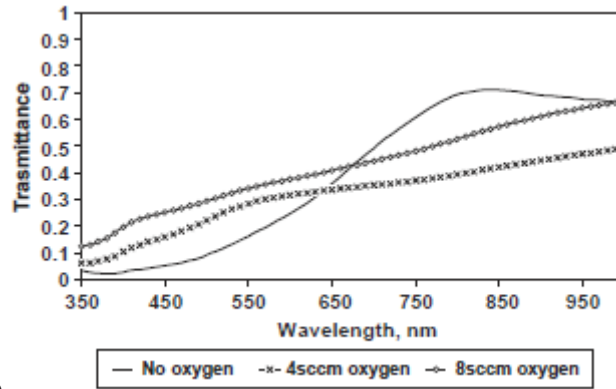
$$\alpha h\nu = A(h\nu - E_g)^{n/2} \quad (3.)$$

by plotting  $(\alpha h\nu)^{n/2}$  versus  $h\nu$ , where  $A$  is a constant,  $n=1/2$  for direct and  $n=2$  for indirect allowed transition. A linear fit of the data to Eq. (3) gives the type of allowed transition and the optical absorption edge ( $E_g$ ).

The plots indicate a direct band gap for both Cu<sub>2</sub>O and CuO, as shown in Fig. 3.2.6 for films deposited in an argon only environment and then annealed in air. Three different band gap values were obtained with 2.24 eV for the pure Cu<sub>2</sub>O phase, 1.78 eV for CuO phase and 2.11 eV for the mixed-phased film. These values are in good agreement with the values reported in the literature for copper oxide films<sup>(4,5,10,25)</sup>.

The transmittance spectra of the as-deposited CuAlO<sub>2</sub> coatings are shown in Fig. 3.2.7. As can be seen, transmittance tended to increase with increasing oxygen flow rate, up to a maximum value of 85% for coating CAO5 with a thickness of 20 nm. Annealing the films under atmospheric conditions at 550 °C for 1 h further increased transmittance. Indeed a peak transmittance of 95% at a wavelength of 600 nm was measured for CAO5. The transmittance spectrum of the annealed film is also included in Fig. 3.2.7.

In the literature the optical absorption edge for copper aluminum oxide thin films for direct allowed transition is reported to be above 3.5 eV<sup>(14–17)</sup>. However, the spectral range of the equipment used in this study was limited and therefore, it was not possible to measure the direct band gap energy. However, using the technique described above, the indirect band gap of the films was estimated to be 1.6 eV for the as-deposited films prepared without additional oxygen flow.



0

Fig. 3.2.5. Optical transmittance spectra of copper oxide thin films deposited at various oxygen flow rates and annealed at 550 °C

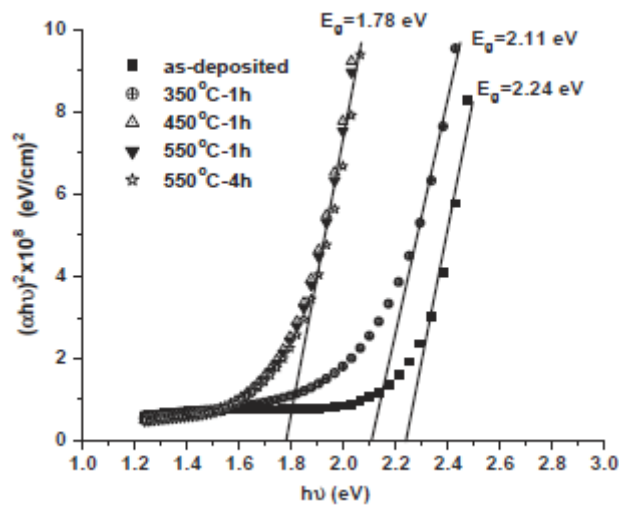


Fig. 3.2.6. Optical band gaps of copper oxide thin films (Coating CO<sub>2</sub>) deposited in an argon-only atmosphere and post deposition annealed at various temperatures and times.

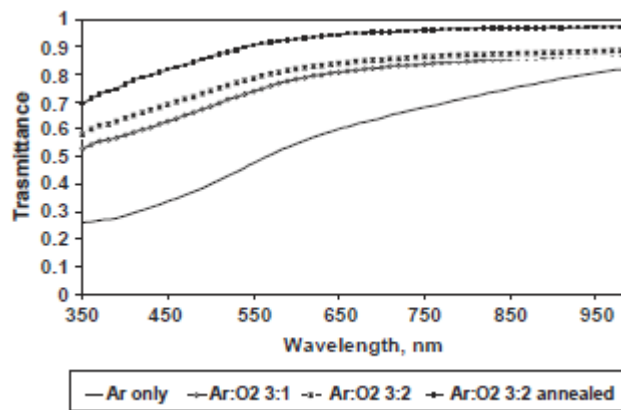


Fig. 3.2.7. Transmittance spectra of copper aluminum oxide films, deposited at various argon : oxygen ratios (annealing conditions:550 °C for 1 h).

### 3.3. Electrical properties

The electrical resistivity of the films was measured using a four-point probe. Several measurements were taken from each sample and an average is reported here with a deviation of less than 10%. For the copper oxide films, resistivity was observed to change with composition and annealing temperature. For example, the electrical resistivity of the Cu<sub>2</sub>O film produced at room temperature with no additional oxygen (sample code CO1) was 412 Ωcm. After annealing at different temperatures, the resistivity changed in a non-regular manner, as listed in Table 4.1, before falling to a value of 24 Ωcm for the phase-pure CuO film annealed at 550 °C for 4 h.

In comparison, the resistivity of the coatings deposited with additional oxygen were significantly lower in the as-deposited condition, with values of 0.25 and 0.30 Ωcm, being obtained for films deposited at 4 and 8 sccm oxygen flow rates, respectively. Following annealing these values increased somewhat, up to values of 5–7 Ωcm for the coatings annealed at 550 °C (see Table 4.1).

The copper aluminum oxide coatings showed very little variation with deposition conditions, with all the coatings having resistivities of the order of 5–10 Ωcm.

## 4. Discussion

This study has demonstrated that dense, defect free, phase pure Cu<sub>2</sub>O, CuO and CuAlO<sub>2</sub> thin films can all be produced by the pulsed magnetron sputtering of loosely packed oxide powder targets. Crystallographic structure and, in turn, the optical and electrical properties of the films, was controlled by varying the working gas composition and the post-deposition annealing conditions. The investigation into copper oxide coatings showed that single-phase cuprite coatings could be deposited by the direct sputtering of a Cu<sub>2</sub>O powder target in an argon-only atmosphere. Introducing additional oxygen into the working gas, or post-deposition annealing of the cuprite films led to the formation of the tenorite phase. Whilst tenorite films produced by the latter route were deposited at a higher rate and revealed a higher degree of crystallinity, those deposited by the former route showed the lowest resistivity. Indeed, the resistivity of these films was considerably lower than values published elsewhere in the literature for CuO films<sup>4,9</sup>. The optical properties of the copper oxide coatings also depended somewhat on the production route, but generally bear favourable comparison with other published data<sup>4,5,10,25</sup>.

The CuAlO<sub>2</sub> coatings produced by sputtering the blended oxide target also demonstrated electrical and optical properties comparable with other published values<sup>1,13–17</sup>. However a major advantage of this technique is the ease of which the target was formed, compared to the complex multi-stage processes used elsewhere. For example, Banerjee et al. produced a CuAlO<sub>2</sub> sputtering target in a process involving heating a mixture of Cu<sub>2</sub>O and Al<sub>2</sub>O<sub>3</sub> powders at 1100 °C for 24 h, during which time the blend was remixed every 6 h. The sintered particles were then reground and hydrostatically pressed into pellets<sup>15–17</sup>. A similarly involved process was used in other studies to produce CuAlO<sub>2</sub> laser ablation targets<sup>1,13</sup>. By comparison, the loosely packed powder targets used here were extremely quick and simple to produce. They also offer the advantage of allowing the target composition to be readily varied, permitting, for example, the effect on film properties of different dopant elements to be investigated<sup>18–20</sup>.

**Table 4.1.** Copper oxide four-point probe resistivity values for as-deposited films and films annealed at various temperatures and times

Sample No.	As-deposited	350 °C (1 h)	450 °C (1 h)	550 °C (1 h)	550 °C (4 h)
CO1 (Ar only)	412 Ωcm	63 Ωcm	222 Ωcm	98 Ωcm	24 Ωcm
CO3 (4 sccm O <sub>2</sub> )	0.24 Ωcm	2.9 Ωcm	3.0 Ωcm	3.7 Ωcm	7.3 Ωcm
CO5 (8 sccm O <sub>2</sub> )	0.30 Ωcm	1.6 Ωcm	1.8 Ωcm	2.9 Ωcm	5.1 Ωcm

## 5. Conclusions

1. Single-phase cuprite films were produced by the pulsed magnetron sputtering of a loosely packed  $\text{Cu}_2\text{O}$  powder target in a rig specifically designed for powder target use.
2. Single-phase tenorite films were also produced either by reactively sputtering this target, or through the post-deposition annealing of the cuprite films.
3. The as-deposited  $\text{Cu}_2\text{O}$  films were found to have a very high optical transmittance in the visible range with up to 95% transmission (film thickness = 100 nm). In comparison, the  $\text{CuO}$  films showed lower transmittance in the visible range, but greater transmittance in the IR range.
4. The optical band gaps obtained from the transmittance and reflectance measurements were 2.44 and 1.78 eV for  $\text{Cu}_2\text{O}$  and  $\text{CuO}$ , respectively.
5. Electrical resistivity measurements as low as  $0.24 \Omega\text{cm}$  were recorded for the  $\text{CuO}$  coatings.
6. Single-phase, strongly textured  $\text{CuAlO}_2$  coatings were also produced by the pulsed magnetron sputtering of a blended  $\text{Cu}_2\text{O}/\text{Al}_2\text{O}_3$  powder target.
7. The transmittance of these films tended to increase with increasing oxygen flow rate, up to a maximum value of 85% at a film thickness of 20 nm. Annealing the films under atmospheric conditions further increased transmittance, up to a peak value of 95% at a wavelength of 600 nm.
8. The indirect band gap was estimated to be 1.6 eV for the as-deposited  $\text{CuAlO}_2$  films and electrical resistivity values were of the order of  $5\text{--}10\Omega\text{cm}$ .
9. The ability to produce high quality  $\text{Cu}_2\text{O}$ ,  $\text{CuO}$  and  $\text{CuAlO}_2$  coatings with good optical and electrical properties in a relatively simple process is an important step-forward in this field and demonstrates the effectiveness of the deposition technique employed here.

## References

- 1) Yanagi H, Inoue S, Ueda K, Kawazoe H, Hosono H. *J Appl Phy*, 2000, 88;4159 .
- 2) Tonooka K, Shimokawa K, Nishimura O. *Thin Solid Films*, 2002;411:129.
- 3) Ray, SC. *Sol Energy Mater Sol Cells*, 2001,68:307.
- 4) Pierson JF, Thobor-Keck A, Billard A. *Appl Surf Sci*, 2003,210:359.
- 5) Balamurugan B, Mehta BR., *Thin Solid Films*, 2001, 396:90.
- 6) Ghosh S, Avasthi DK, Shah P, Ganesan V, Gupta A, Sarangi D, Bhattacharya R, Assmann W. *Vacuum*, 2000,57:377.
- 7) Yoon KH, Choi WJ, Kang DH., *Thin Solid Films*, 2000,372:250.
- 8) Santra K, Sarker CK, Mukherjee MK, Ghosh B., *Thin Solid Films*, 1992,213:226.
- 9) Nair MTS, Guerrero L, Arenas OL, Nair PK., *Appl Surf Sci*, 1999,213:143.
- 10) Oral AY, Mensur E, Aslan MH, Basaran E., *Mater Chem Phys*, 2004,83:140.
- 11) Muthe KP, Vyas JC, Narang SN, Aswal DK, Gupta SK, Bhattacharya D, Pinto R, Kothiyal GP, Sabharwal SC., *Thin Solid Films*, 1998,324:37.
- 12) Maruyama T., *Sol Energy Mater Sol Cells*, 1998, 56:85.
- 13) Kawazoe H, Yasukawa M, Hyodo H, Kurita M, Yanagi H, Hosono H. *Nature* 1997,389:939.
- 14) Kawazoe H, Yanagi H, Ueda K, Hosono H, *Bull MRS.*, 2000, August: 28.
- 15) Banerjee AN, Kundoo S, Chattopadhyay KK., *Thin Solid Films*, 2003,440:5.
- 16) Banerjee AN, MaityR, Chattopadhyay KK., *Mater Lett*, 2003,58:10.
- 17) Banerjee AN, Chattopadhyay KK., *Appl Surf Sci*, 2004,225:243.
- 18) KellyPJ, Zhou Y, Postill A., *Thin Solid Films*, 2003,426:111.
- 19) Zhou Y, KellyPJ, Postill A, *Proceedings of the seventh International Symposium on Sputtering and Plasma Processes (ISSP 2003)*, Kanazawa, Japan, June 2003. p. 145–148.
- 20) Zhou Y, KellyPJ, Postill A, Abu-Zeid O, Alnajjar AA. *Thin Solid Films*, 2004,447–448:33.
- 21) Zhou Y, Kelly PJ. *Thin Solid Films*, 2004,469–470:18. E.M. Alkoy, P.J. Kelly, *Vacuum* 79 (2005) 221–230 229
- 22) KellyPJ, Zhou Y, Pilkington RD, Arnell RD., *Surf Eng*, 2004,20(3):157.

- 23) KellyPJ, Zhou Y, Hisek J, Pilkington RD, *Proceedings of the SVC 47<sup>th</sup> annual technical conference*, Dallas, 2004. p. 295–9.
- 24) Audronis M, KellyPJ, Arnell RD, Valiulis AV, *Pulsed magnetron sputtering of chromium boride films from loose powder targets. Surf Coat Technol*, in press.
- 25) Mathew X, Mathews NR, Sebastian PJ., *Sol Energy Mater Sol Cells*, 2001,70:277.